



**HAL**  
open science

## Electroactivity of a starburst hole-transport material in Langmuir–Blodgett films. Solid state effects and intervalence charge transfer

Vicente Parra, Teodosio Del Caño, María L Rodríguez-Méndez, José A de Saja, Marcel Bouvet, Yasuhiko Shirota

### ► To cite this version:

Vicente Parra, Teodosio Del Caño, María L Rodríguez-Méndez, José A de Saja, Marcel Bouvet, et al.. Electroactivity of a starburst hole-transport material in Langmuir–Blodgett films. Solid state effects and intervalence charge transfer. *Physical Chemistry Chemical Physics*, 2007, 9 (18), pp.2266-2273. 10.1039/b618509f . hal-02275462

**HAL Id: hal-02275462**

**<https://hal.science/hal-02275462>**

Submitted on 30 Aug 2019

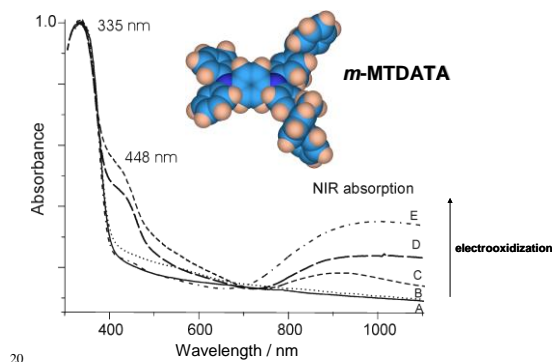
**HAL** is a multi-disciplinary open access archive for the deposit and dissemination of scientific research documents, whether they are published or not. The documents may come from teaching and research institutions in France or abroad, or from public or private research centers.

L'archive ouverte pluridisciplinaire **HAL**, est destinée au dépôt et à la diffusion de documents scientifiques de niveau recherche, publiés ou non, émanant des établissements d'enseignement et de recherche français ou étrangers, des laboratoires publics ou privés.

Lorsqu'un écrit scientifique issu d'une activité de recherche financée au moins pour moitié par des dotations de l'État, des collectivités territoriales ou des établissements publics, par des subventions d'agences de financement nationales ou par des fonds de l'Union européenne est publié dans un périodique paraissant au moins une fois par an, son auteur dispose, même après avoir accordé des droits exclusifs à un éditeur, du droit de mettre à disposition gratuitement dans un format ouvert, par voie numérique, sous réserve de l'accord des éventuels coauteurs, la version finale de son manuscrit acceptée pour publication, dès lors que l'éditeur met lui-même celle-ci gratuitement à disposition par voie numérique ou, à défaut, à l'expiration d'un délai courant à compter de la date de la première publication. Ce délai est au maximum de six mois pour une publication dans le domaine des sciences, de la technique et de la médecine et de douze mois dans celui des sciences humaines et sociales.

## Graphical abstract

The fundamental **electrochemical** properties of unprecedented **Langmuir-Blodgett** films of ***m*-MTDATA** are analyzed to support why it is one of the most **efficient hole-transport** materials in OLEDs applications.



**To cite this paper:** V. Parra\*, T. Del Cano, M. L. Rodriguez-Mendez, J. A. De Saja, M. Bouvet, Y. Shirota, "Electroactivity of a starburst hole-transport material in langmuir-blodgett films. Solid state effects and intervalence charge transfer", *Phys. Chem. Chem. Phys.*, 9, 2266-2273, **2007**.

## Electroactivity of a Starburst Hole-Transport Material in Langmuir-Blodgett films. Solid State Effects and Intervalence Charge Transfer

Vicente Parra\*<sup>a</sup>, Teodosio Del Caño<sup>b</sup>, María L. Rodríguez-Méndez<sup>a</sup>, José A. De Saja<sup>b</sup>, Marcel Bouvet<sup>c</sup> and Yasuhiko Shirota<sup>d</sup>

<sup>a</sup>Dpto. de Química Física y Química Inorgánica. E.T.S. Ingenieros Industriales. University of Valladolid, Pº del Cauce s/n. 47011 Valladolid (Spain). \*E-Mail: vparr@eis.uva.es

<sup>b</sup>Dpto. Física de la Materia Condensada, Facultad de Ciencias, University of Valladolid. Prado de la Magdalena s/n 47005 Valladolid (Spain).

<sup>c</sup>Lab. Chimie Inorganique et Matériaux Moléculaires-CNRS UMR 7071. Université Pierre et Marie Curie-Paris 6. Paris (France).

<sup>d</sup>Department of Environmental and Biotechnological Frontier Engineering, Fukui University of Technology (Japan).

Here we report on the electroactivity properties of Langmuir-Blodgett (LB) films of the hole-transport molecule 4,4',4''-tris[3-methylphenyl(phenyl)amino] triphenylamine (*m*-MTDATA). Fairly stable Langmuir films at the air-water interface are accomplished, despite the non-amphiphilic character of the molecule. The Reflection-Absorption Infrared Spectroscopy (RAIRS) and Fourier Transform Infrared (FT-IR) analysis revealed that the molecules arrange with no neat preferential orientation, in agreement with the amorphous glassy nature of this starburst molecule. However, there is a tendency of the molecules to organize in a more planar conformation due to the intermolecular stacking induced by the LB technique. On the other hand, the fundamental electrochemistry (by Cyclic Voltammetry, CV) of the films is also analyzed. The CV studies of both solution and films reveal that both the solid

---

state and the electrolyte's anions clearly affect the m-MTDATA's electroactivity, exhibiting a unique and broad redox process instead of the two reversible oxidations observed in solution. The oxidization mechanism is discussed. Finally, the spectroelectrochemistry studies evidence that the oxidization of the films leads to new absorption bands, among which it should be pointed up the emerging bands in the NIR region ascribed to intervalence charge transfer (IVCT) between the generated aminyl radical cations.

## 1. Introduction

Organic semiconductors have emerged in the last decade as main active components in practical thin films devices as photovoltaic cells, light emitting displays, field-effect transistors, sensors and other electronic devices<sup>1-3</sup>. Within the large variety of organic semiconductors, amorphous molecular materials or "molecular glasses" have found successful application for use in organic electroluminescent devices (OLEDs) and other applications as photovoltaic, photochromic and resist materials<sup>4</sup>. The reason of this rich variety of applications is their facility to form smooth, uniform, isotropic, and in certain cases transparent thin films by evaporation or spin-coating from solution. In particular, 4,4',4''-tris[3-methylphenyl(phenyl)amino]triphenylamine (m-MTDATA) is widely known to be an excellent hole-transport material that has been extensively and successfully used in OLEDs designing<sup>5,6</sup>.

Recently, one of the authors of the present work has studied the influence of the method of thin film preparation in the performance of OLEDs using m-MTDATA as hole injector<sup>7</sup>. Thus, it is motivating to study the properties of thin films fabricated using alternative techniques such as Langmuir-Blodgett, focusing in their electrochemical and spectroelectrochemical behavior.

The LB technique has been mainly used in the fabrication of thin films of molecular materials of amphiphilic nature or with high planarity that can easily form ordered films<sup>8</sup>. However, few attempts have been carried out to prepare LB films of non-amphiphilic polymers<sup>9</sup>, characterized by the absence of molecular order, or non-planar molecules as fullerene<sup>10</sup>, coordination complexes<sup>11</sup>, etc. Thus, in this line, although m-MTDATA results to be a non-amphiphilic starburst molecule, its extended  $\pi$ -conjugated system might allow a high enough intermolecular coupling compatible with the LB

technique. In addition, the fabrication of this kind of molecular films is useful in applications where the film thickness should be controlled at a nanometric level or in devices where the physicochemical process takes place at the film surface, as for instance, in sensor units<sup>12</sup>.

Therefore, the reasons of using the LB technique are, on one hand, the skills offered by this approach when one wants to attain homogeneous and controlled films. On the other hand, we contributed on the fundamental research on LB films, regarding the particular structural features of m-MTDATA.

In addition, the application of fundamental electrochemical methods to survey the oxidative behavior of materials with inherent hole-transport properties can be extremely useful<sup>13</sup>. Using voltammetric techniques such as CV, it is feasible to elucidate features such as the number of electron transfer processes involved in the redox steps, the active sites present in the skeleton's molecule, and their kinetic and thermodynamic properties, among other practical information as the estimation of optical bandgaps<sup>14,15</sup>. Indeed, the electrochemical characterization of m-MTDATA has been carried out yet in solution<sup>16</sup>. However, since the practical applications in devices take place in the solid state, it would be of great interest to exploit the CV behavior in molecular films as LB multilayers, which are closely related to the functionality of molecular materials in Organic Electronics purposes.

Finally, and according to the important role played by this starburst triphenylamine molecules in OLEDs applications<sup>4,17-19</sup>, we studied the spectroelectrochemical behavior of the films, which, by integration with the results from the electrochemical experiments, can provide a powerful source of information in order to analyze the electroactive properties of m-MTDATA in thin films, as it does when

playing the role of hole-transport material in molecular electronic devices.

Triarylamine derivatives bringing a number of linked  $\pi$ -bridged phenylamine groups are materials that lead to mixed-valence states once oxidized. Studies dealing with mixed-valence organic materials have not been traditionally performed if we compare with those of metal-bonded or metal-conjugated compounds<sup>20</sup>. Thus, in particular, the analysis of the spectroelectrochemical behavior of m-MTDATA in LB thin films state constitutes a profitable experiment to support its usage as functional material in electroluminescent devices. Moreover, this kind of experiments are likely to be integrated with the electrochemical analysis previously discussed, and then leading to a valuable source of information regarding the electroactive properties of this molecule in thin films, i.e. the state used in Organic Electronics applications.

There are a very scarce literature devoted to spectroelectrochemical studies of this sort of materials in solid state, and those existing deal with electropolymerized films<sup>18,21</sup>. However, none study has been performed in films built using electroless approaches as the LB technique, that is, in films built by pure solid state intermolecular interactions.

## 2. Experimental

### 2.1 Materials.

m-MTDATA was synthesized according to the reported procedure<sup>16</sup>. Dichloromethane (CH<sub>2</sub>Cl<sub>2</sub>, HPLC grade, purchased from Aldrich), KCl, KClO<sub>4</sub>, tetrabutylammonium perchlorate (TBAP, 99% Aldrich) and ferrocene (Fluka) were used as received. For solid state electrochemistry, water solvent was distilled and subsequently passed through a Millipore Milli-Q system to attain ultrapure quality (18.2 M $\Omega$ .cm resistivity).

### 2.2 LB films and LB electrodes fabrication.

The thin films were fabricated using a KSV 5000 LB trough equipped with a Wilhelmy plate to measure the surface pressure changes. The m-MTDATA was dissolved in CH<sub>2</sub>Cl<sub>2</sub> at a concentration of 1.1x10<sup>-4</sup> mol.L<sup>-1</sup>. A total

volume of 350  $\mu$ l was spread with a Hamilton microsyringe onto ultrapure distilled Millipore Milli-Q water, maintained at 18 °C. Monolayer characterization and isotherm stability tests were carried out. After evaporation of the solvent (20 minutes), the floating molecules were compressed at 10 mm.min<sup>-1</sup> speed. The layers were then transferred to glass, gold mirrors and ITO/glass substrates at 5 mm.min<sup>-1</sup> speed when a target surface pressure of 18 mN.m<sup>-1</sup> was reached (within the solid phase of the Langmuir film). The thin films were fabricated using Z-deposition (i.e. transferred only during substrate's upstroke). 18 Monolayers were transferred to the different substrates. This entails the accomplishment of a practical film thickness, representative of that used in device's designing.

For the fabrication of the m-MTDATA LB-based electrodes used in the electrochemical and spectroelectrochemical experiments, glass slides (2.5 x 1 cm<sup>2</sup>) coated with ITO (150  $\Omega$ /sq sheet resistance) were used as substrates, being initially cleaned in pure acetone and ultrasonicated in Millipore MilliQ water for 5 minutes. The metallic contacts were ensured with silver paste and fixed by adding an epoxy resin on top of them.

The gold films (50 nm thick) used as substrates for Reflection-Absorption Infrared Spectroscopy (RAIRS) measurements were prepared by high vacuum deposition (BALZERS SCD004) over microscope glass slides.

### 2.3 Thin film characterization and electrochemical measurements.

The UV/Vis/NIR spectra of films were recorded using a double beam SHIMADZU 1603 spectrophotometer (wavelength range 300-1100 nm). RAIRS spectra were recorded using a Nicolet Magna IR 760 Spectrometer equipped with a DTGS detector. The RAIRS spectra were recorded at an incident angle of 80°. The material was also dispersed in KBr powder to produce a pellet which transmission infrared provides a random spatial distribution of dynamic dipoles. Therefore, it can be considered as reference in molecular organization studies. All spectra were collected using a resolution of 4 cm<sup>-1</sup>, and the

mean of 256 scans was obtained. The sample chamber was systematically purged using dry N<sub>2</sub> before data collection, to minimize the atmospheric interferences.

Cyclic voltammetry (CV) of LB films were performed using a potentiostat/galvanostat EG&G PARC mod. 263 at controlled temperature (20 °C). We employed a three electrode-cell configuration consisting of a Pt plate (surface: 1.5 x 1 cm) as the auxiliary electrode, an Ag/AgCl|KCl saturated as reference electrode, and LB thin films of m-MTDATA coating ITO/glass substrates (surface: 2.5 x 1 cm) as working electrodes. To avoid a possible effect of oxidization of m-MTDATA in presence of oxygen, all solutions were previously purged using dry N<sub>2</sub>. For CV experiments in organic solution, the potentials were measured against the same aqueous-based reference electrode, but the peaks were calibrated with an external standard, the ferrocene/ferrocenium (Fc/Fc<sup>+</sup>) redox system, at analogous conditions (0.1 mol.L<sup>-1</sup> TBAP in CH<sub>2</sub>Cl<sub>2</sub>). The working electrode was a Pt disk (1 mm diameter) and the auxiliary electrode, a Pt wire.

The potential scans were applied in oxidative sense, from negative potentials (-0.75 or -0.20 V, corresponding to voltages separated from the m-MTDATA's electroactivity) to 1.3 V, and finishing at the original potential values. The sweep rates ranged from 20 to 500 mV.s<sup>-1</sup> depending on the aim of each experiment.

The spectroelectrochemistry was carried out by oxidizing the films at fixed potentials by both CV and chronoamperometry, then recording the subsequent UV/Vis/NIR spectra independently.

### 3. Results and discussion

#### 3.1 Langmuir and Langmuir-Blodgett Films.

Reproducible surface pressure ( $\Pi$ )-area isotherms of the m-MTDATA floating monolayers were obtained, being characterized by the formation of a well-defined solid phase as shown in Figure 1. As it is observed, the surface pressure starts to raise at area-per-molecule values of ca. 110 Å<sup>2</sup>. Then, a monotonous stiff rising in  $\Pi$  starts near 8 mN.m<sup>-1</sup>. This part of the isotherm can be attributed to the liquid-solid

phase transition due to the increasing  $\pi$ - $\pi$  intermolecular interaction in the floating film. The area-per-molecule value extrapolated to  $\Pi = 0$  for the Langmuir film - the "mean molecular" area - extracted from the sharpest portion of the isotherm results to be 76 Å<sup>2</sup>. Finally, at a pressure of ca. 25 mN.m<sup>-1</sup> (molecular area of 45 Å<sup>2</sup>), a slight slope change occurs, which is ascribed to the beginning of the Langmuir film's collapse.

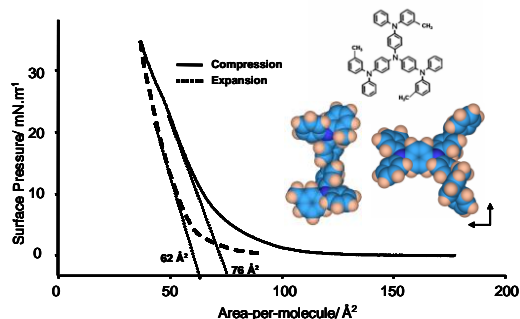


**Fig.1.-**  $\Pi$ -A Isotherm compression-expansion cycle of the m-MTDATA Langmuir film registered at 18 °C. Upper inset: molecular structure of m-MTDATA; lower inset: molecular models created by molecular mechanics geometry optimization (MOPAC/AM1) of two suitable projections of m-MTDATA at the water subphase (defined by the plane formed by the arrows). On the left ("2-linked" configuration), the surface area is ca. 160 Å<sup>2</sup>, whereas on the right ("3-linked" configuration), the area-per-molecule would be no lower than 300 Å<sup>2</sup>. In both cases, the figures are represented considering 100% Van der Waals radii.

Although m-MTDATA is non-amphiphilic and non-planar, this  $\Pi$ -A isotherm behavior indicates a strong film cohesion, not high film rigidity and a good stability on the water subphase. The found extrapolated area-per-molecule value (to  $\Pi = 0$ ) is markedly lower than those that would exhibit two highly plausible projections of the molecule in the water subphase (inset of Figure 1), 160 Å<sup>2</sup> and 300 Å<sup>2</sup>, respectively. The estimation has been performed using molecular mechanics geometry optimization (MOPAC/AM1), taking the molecular models as basic geometrical forms. This suggests the formation of a non-

monomolecular film at the air-water interface. In any case, one can observe that the extended  $\pi$ -conjugated electronic system allows high enough stacking between adjacent molecules, leading to the formation of the clear solid phase in the isotherm. Moreover, in order to study the degree of reversibility of the interactions between the film-forming molecules, some compression-expansion studies were carried out at  $\Pi = 35$  mN.m<sup>-1</sup> (from 0 to  $\Pi$  mN.m<sup>-1</sup>, then the inverse process), over the collapse point. As it is also noticed in Figure 1, the corresponding first expansion cycle shows an extrapolated molecular area to zero surface pressure of 62 Å<sup>2</sup> indicating certain, but not severe, degree of hysteresis.

In summary, although the m-MTDATA floating layer on pure water might not be a true monomolecular layer, the extracted area-per-molecule value, and the moderate hysteresis, indicates that this starburst molecule accommodates well-enough in a floating layer structure, forming a non-monomolecular layer but permitting the transfer onto solid substrates. Regarding this process, the transfer ratios varied from 1.2 from the first upstroke to 0.6 for the last layer transferred, in agreement with the non-aphilic character of the compound.

### 3.2 Fourier Transform Infrared (FTIR) analysis.

In this study, Polarization IR spectroscopy was used to determine the molecular arrangement within the m-MTDATA LB film. Reflection-absorption Infrared spectroscopy (RAIRS) profits from the perpendicular polarization of the electrical field at the nodal point on the reflecting surface plane. Therefore, the intensity of the vibrational modes with dynamic dipole components perpendicular to the surface will be enhanced, while those parallel to the surface will be suppressed<sup>23,24</sup> (i. e., a “surface selection rule”). Pellet (bulk) transmission spectrum, where the material is dispersed in a KBr matrix, i.e. random spatial distribution of dynamic dipoles, is used as reference. Thus, by comparison of the relative intensity of the vibrational modes in transmission KBr and RAIRS spectra, information about the molecular organization over the substrate can be extracted<sup>25</sup>.

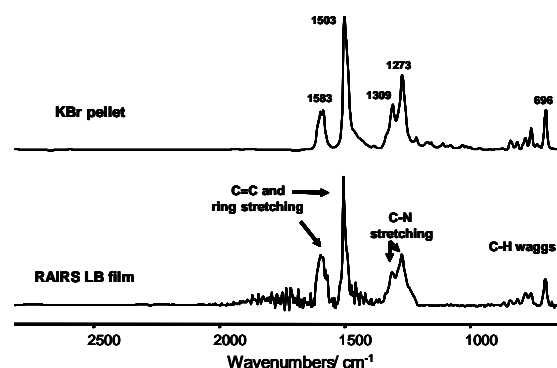


**Fig.2.-** FT-IR transmission spectrum of a KBr pellet and RAIRS spectrum of the m-MTDATA LB film.

In Figure 2, the LB film RAIRS and KBr pellet spectra of the m-MTDATA are shown. Table 1 also collects some quantitative data regarding the relative intensities and assignments of the bands. The main vibrational components of the KBr infrared transmission spectrum are closely related to the triphenylamine spectral patterns and can be summarized as follows: C-H wagging modes centered at 696 and 751 cm<sup>-1</sup>, the C-N stretching modes observed at 1273 and 1309 cm<sup>-1</sup>, the C=C stretching modes at 1503 cm<sup>-1</sup>, the C-C stretching mode at 1583 and 1592 cm<sup>-1</sup>. In this spectrum, the most intense vibrational band results to be the C=C stretching mode at 1503 cm<sup>-1</sup>, followed by the C-N stretching mode observed at 1273 cm<sup>-1</sup>. At first glance, the thin film m-MTDATA RAIRS spectrum shows a similar profile that could be ascribed to an random distribution of dipoles, and thereby, the absence of a preferential molecular alignment, in agreement with the amorphous nature of m-MTDATA.

However, a detailed analysis of the relative intensities highlights certain differences between spectra. In the RAIRS, the C=C and C-C stretching modes become more prominent, whereas the C-N stretching modes and the C-H wagging modes show lower intensities if we compare with the pellet spectrum. These changes in relative intensities might be correlated with a close packing of the triphenylamine groups of adjacent m-MTDATA molecules, which is enhanced due to the LB technique. It is known that this starburst molecule owns a non-planar shape, and the introduction of the methyl

415 substituents at the meta-position of the phenyl  
 group favors the amorphous glassy state<sup>16</sup>.  
 Then, despite one can deduce the absence of a  
 neat preferential molecular orientation in thin  
 films, and according to the relative intensities of  
 420 the C-N stretching and C-H wagging modes in  
 the LB film RAIRS spectrum with respect to the  
 randomly arranged KBr pellet, this particular  
 solid state supports the reorganization of the m-  
 MTDATA molecules in a more planar  
 425 conformation, a practical fact that would entail  
 an improvement of the electron conjugation all  
 along the starburst skeleton.

**Table 1.-** Wavenumbers of characteristic  
 430 vibrational modes of m-MTDATA observed in  
 the FT-IR spectra in thin film (RAIRS) and KBr  
 pellet. The relative absorbance's intensities are  
 referred to the strongest peak in the pellet  
 spectrum.

Vibrational modes	KBr pellet	RAIRS LB film	Assignments
Wavenumber / cm-1	Irelative	Irelative	
1584	0.29	0.38	C-C phenyl stretching
1503	1	1	C=C phenyl stretching
1309	0.35	0.24	C-N stretching
1271	0.46	0.38	C-N stretching
696	0.3	0.2	C-H wagging

### 3.3 Electrochemical studies.

#### 3.3.1 CV of m-MTDATA in solution.

A 10<sup>-3</sup> mol.L<sup>-1</sup> CH<sub>2</sub>Cl<sub>2</sub> solution of m-  
 440 MTDATA was examined by CV in order to  
 study its oxidation properties. Since the reference  
 electrode was Ag/AgCl|KCl saturated and we  
 used CH<sub>2</sub>Cl<sub>2</sub> as organic solvent, the ferrocene  
 (Fc) electroactivity was measured at equal  
 445 conditions, in order to have an external reference  
 (E<sub>1/2</sub> vs. Ag/AgCl = 0.57 V). Figure 3 represents  
 the voltammograms of m-MTDATA in a  
 CH<sub>2</sub>Cl<sub>2</sub> solution. In agreement with the  
 electrochemical behavior of m-MTDATA  
 450 previously found in solution but in other  
 conditions<sup>16</sup>, two reversible processes can be  
 observed at E<sub>1/21</sub> = 0.43 V and E<sub>1/22</sub> = 0.79 V

vs. Ag/AgCl (-0.14 V and 0.22 V vs. Fc,  
 respectively). These data in solution correlate  
 455 well with those published by Shirota et al., where  
 the first oxidation half-wave potential was found  
 at 0.06 V vs. Ag/Ag<sup>+</sup> (0.01 mol.L<sup>-1</sup>), and an  
 ionization potential (IP) of 5.1 eV was extracted.  
 Here, taking into account the value E<sub>1/21</sub> = -0.14  
 460 V vs. Fc and the theoretical value of Fc, -4.8 eV  
 vs. vacuum level, the estimated IPs would be 5  
 eV. This result highlights the low ionization  
 potential of m-MTDATA, in agreement with its  
 known electron donating ability. The feasible  
 465 molecular centres that can be oxidized are the  
 nitrogen atoms of the triphenylamine groups.  
 Thus, those peaks are in agreement with the  
 occurrence of two one-electron oxidation steps.  
 The SWV diagram shown in the inset of Figure 3  
 470 supports this statement, where two well-defined  
 and narrow peaks are observed at values  
 comparable to the half-wave potentials observed  
 in CV. Furthermore, the sensible difference  
 between first and second oxidation processes  
 475 ( $\Delta E = E_{1/22} - E_{1/21} = 360$  mV at the used  
 experimental conditions) indicates that p-  
 phenylamine redox centers are effectively  
 connected, thus stabilizing the positive charge all  
 along the starburst skeleton upon  
 480 oxidation<sup>26,27</sup>.

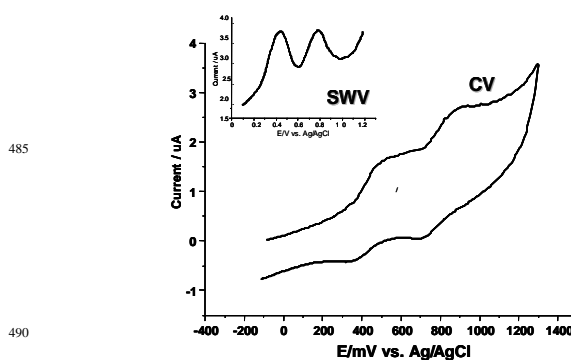


**Fig.3.-** Cyclic voltammogram of m-MTDATA  
 (10 mM) in CH<sub>2</sub>Cl<sub>2</sub> with TBAP as the  
 supporting electrolyte (sweep rate: 100 mV.s<sup>-1</sup>).  
 Inset: Square Wave Voltammogram. Conditions:  
 495 Frequency: 15 Hz; Potential Height: 100 mV;  
 Potential scan increment: 5 mV.

#### 3.3.2 CV of LB films in KCl aqueous solution.

The electrochemical response of the m-  
 500 MTDATA LB electrode in KCl and in KClO<sub>4</sub> is

reported in Figure 4. Figure 4a shows the two first cycles of an 18-layer LB film, which display an oxidation process defined by a unique redox couple. It is observed the appearance of an anodic peak from the second cycle, accompanied to the corresponding cathodic couple, which is slightly shifted with respect to the first one. The anodic potential locates at 0.95 V and the cathodic at 0.49 V, which means  $E_{1/2} = 0.77$  V. This well-defined redox couple, with an icathodic/ianodic ratio near 1, suggests that the electrochemical step is quasireversible.

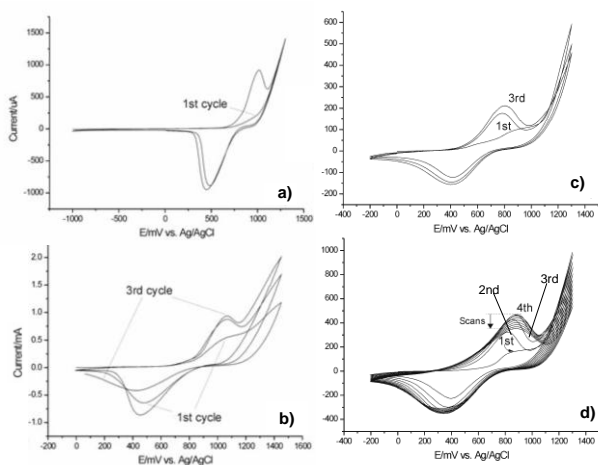


**Fig.4.-** Cyclic voltammograms of a 18-layer LB film immersed in a 0.1 mol.L-1 aqueous KCl solution; a) First two cycles starting from 0 V; b) first three scans in the subsequent experiment. Cyclic voltammograms of several molecular films immersed in a 0.1 mol.L-1 aqueous KClO4 solution; c) 18-layer LB film. Three first cycles. Sweep rate: 100 mV.s-1; d) 18-layer LB film, 12 times cycled at the same conditions.

In Figure 4b, the subsequent three cycles after the initial two cycled scanning are presented to allow the stability of the film in KCl to be checked. As is observed, consecutive scanning produces evident changes in the CV, which mainly occur in the cathodic waves. Herein, the peak shifts to lower potentials and current values vary, besides the occurrence of a clear loss of shape.

### 3.3.3 CV of LB films in KClO4 solution.

It can be expected that during the films' oxidization, the electrolytic anions will diffuse into the film to maintain the electroneutrality of the system. For this reason, the use of different counteranions should help to elucidate the nature of the oxidization's mechanism.

In order to evaluate the role of the electrolytic solution in the electrochemical properties of the films of m-MTDATA, they were immersed in 0.1 mol.L-1 KClO4 and the results were compared to those obtained by using KCl. In case of ClO4-, the hydrated energy of this counteranion is markedly lower (i.e. more hydrophobic) than that of Cl- ( $-\Delta G_{\text{solvation}} = 214$  KJ.mol-1 vs. 347 KJ.mol-1, respectively)28. Thus, it is possible to acquire useful information regarding the affinity of the film to both anions during the oxidization. Figure 4c illustrates the CV diagrams of a LB film in a 0.1 mol.L-1 KClO4 solution. Here, the oxidation and reduction processes at the second cycle appeared at 0.79 V and 0.40 V (i.e.  $E_{1/2} = 0.59$  V). These values, together with the almost found 100% peak currents ratio are also indicative of a quasireversible redox reaction. However, the response of a LB film polarized in KClO4 differed noticeably to that in KCl. On one hand, films immersed in KClO4 are much more easily oxidized (there is a cathodic shift of 180 mV). On the other hand, the electrolyte also plays an important role in the reproducibility of the successive cycles. Figure 4d illustrates this phenomenon. It represents a CV diagram consisting of 12 consecutive cycles from -0.2 to 1.3 V of the LB film cycled in KClO4. During the three first cycles, an increase of the current of both the anodic and cathodic waves is observed. Simultaneously, a slight separation of the anodic and cathodic peaks occurs. Afterwards, when additional scans were applied, the peaks registered were highly reproducible (the peaks location was visibly kept up). This points out that the film's electrochemistry in the perchlorate-based solution is more reversible and stable than in KCl electrolyte.



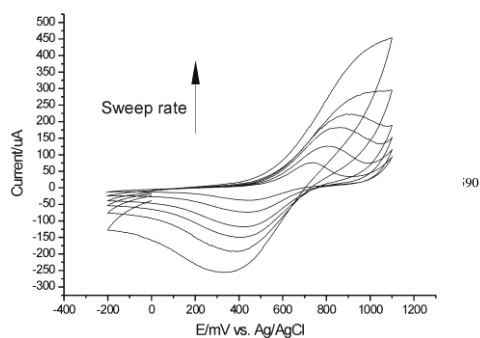


**Fig.5.-** Cyclic voltammograms registered at 20, 50, 100, 150, 200, 250 and 500 mV.s<sup>-1</sup> of a m-MTDATA LB film immersed in a 0.1 mol.L<sup>-1</sup> aqueous KClO<sub>4</sub> solution.

### 3.3.4 Redox reaction rate.

The dynamics of the oxidization of the m-MTDATA films was examined by analyzing the influence of the sweep rate (20, 50, 100, 150, 250, 500 mV/s) in the peak features of the LB films (Figure 5, perchlorate-based solution). As a result, when sweep rate increases, besides the expected increasing of peak's currents, the appearance of raising diffusion tails in both anodic and cathodic signals agrees with the occurrence a slow electron transfer electrode reaction. Likewise, in case of the anodic process, there is a highly fitted linear relation between the peak's current and the square root of the sweep rate ( $v^{1/2}$ ), giving a coefficient of regression of  $r^2 = 0.999$  ( $r^2 = 0.970$  for current vs.  $v$ ). Regarding the cathodic waves, values of  $r^2 = 0.998$  vs.  $v^{1/2}$ , and  $r^2 = 0.958$  vs.  $v$  were found. Thus, these trends support the envisaged slow redox kinetics, being the process mainly governed by the diffusion of the electrolyte into the film, more than a mechanism typical of surface-confined species.

### 3.3.4 Solid state (LB) electrochemical behavior. Discussion

Some interesting features are revealed after analyzing the voltammetric behavior of m-MTDATA in LB films, namely i) the appearance of an unique, broad and non-Nernstian oxidation process in LB films instead of the two well defined redox activities observed in solution; ii) a diffusion-controlled, then rather slow redox mechanism and iii) a noticeable

influence of electrolyte's anions in the oxidation process. First, to explain such outcomes, issues as the solid state effects in the thin solid film, the different solvent-based solutions and sizes of the hydrated electrolyte's anions are key factors.

As it was introduced above, it is expected that the electrooxidation of m-MTDATA occurs in the sites with the highest density of charge of the starburst skeleton, namely the nitrogen atoms of the triphenylamine groups. The molecule owns four of them (cf. inset of Figure 1), but the fact that only one and broad peak was observed may indicate a noticeable influence of the adjacent molecules, suggesting the creation of an equivalent charged state in the stacked molecular film. This unique process, according to their features, namely potential values comparable to the two monoelectronic peaks observed in solution, its fashion (large separation of peaks and width) and the slow kinetics behavior, could be related to the formation of not only aminyl radical cations, but also dications<sup>29,30</sup>. Besides, the electrochemically p-doped film would be somehow stabilized by delocalization of the electron density as a result of solid state surrounding and the favored planarity of the m-MTDATA's cores in LB film state (i.e. improved electron conjugation)<sup>31</sup>.

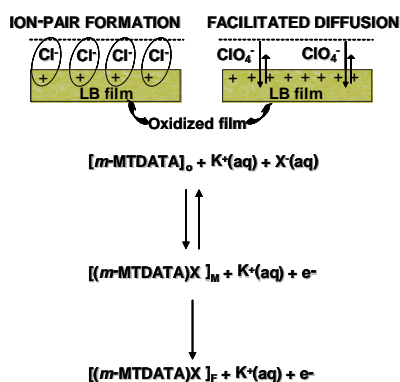


**Fig.6.** Schema illustrating a general mechanism of the m-MTDATA in LB films oxidation (simplified to an one-electron process) by successive potential scans, integrating both the effects of solid state charge delocalization and that of the behavior of electrolyte's counterions (X<sup>-</sup>). The lower hydration energy of ClO<sub>4</sub><sup>-</sup> favors it to ingress and egress easier than Cl<sup>-</sup>. O:

---

original film; M: structurally modified film; F:  
final film.

685

In order to compare the voltammetric behavior in both molecular environments (solution and LB film) and taking into consideration the known hole-hopping charge transport properties phenomenon of m-MTDATA, one can allude to the Marcus theory for the charge transfer<sup>30</sup>. According to this semi-classical theory, the kinetics of the charge transfer is related to the molecule's reorganization energy after formation of radical cations and geometric relaxation. This parameter is defined as the sum of an intramolecular (vibronic) factor - structural changes in the equilibrium structures during the self-exchange charge transfer process  $\text{Molecule}^+ + \text{Molecule} \leftrightarrow \text{Molecule} + \text{Molecule}^+$  - and other attributed to environmental effects (solvent polarity, aggregation state, etc.). As a result, it is obvious that these two terms will contrast manifestly between the CH<sub>2</sub>Cl<sub>2</sub> solution and LB thin film state, either by the oxidization process depending on the solvent-based electrolyte solution or by the relaxation phenomenon after formation of the radical cations in the  $\pi$ - $\pi$  interacting molecular film.

710

On the other hand, it should be also pointed out the effect of the anion's electrolyte in the oxidization mechanism of m-MTDATA LB films, according to the different redox behavior observed, in terms of stability and reversibility, depending on the presence of the hydrated chloride (Cl<sup>-</sup>aq) or perchlorate counterions (ClO<sub>4</sub><sup>-</sup>aq) in the diffusion-layer near the electrode. In both cases, in the first electrooxidative potential scan, there is evidence of no (or rather weak, in case of perchlorate) oxidization peak of the m-MTDATA's multilayer. This indicates that the surface of the film needs to be unlocked to allow the ingress of the counterions to electroneutralize the locally created positive charges (process supported by the prominent cathodic peak in the corresponding reverse scan). In particular, when Cl<sup>-</sup>aq takes action, there is a sensible variation, i.e. different current values and peak shifting at lower anodic potentials, in the electroactivity during the

730

reverse reduction scans. This behavior is likely to be associated to a strong ion-pair formation of chlorides at the film surface (Figure 6).

735

In contrast, this trend is not followed in case of ClO<sub>4</sub><sup>-</sup>aq, anion that makes the electron transfer more reversible and stable. This is likely to be explained in terms of its larger hydrophobicity (i.e. lower hydration energy), which allows it to diffuse (ingress and egress) easily into the film<sup>26</sup>. Nonetheless, herein, the slightly loss in the peak currents ratio (icathodic/ianodic) during consecutive cycling (Figure. 4d), such an outcome also exhibited in the CV diagrams at different sweep rates (Figure. 5), agrees well with the occurrence of a fairly rapid chemical reaction following the oxidization of m-MTDATA molecules.

740

745

The diffusion of charged mass is suggested to be associated to the efficient interconnection between the starburst molecules into the packed film, which permits the renewal of the oxidized surface in a simultaneous way to that of the ion's entrance.

755

### 3.4 Spectroelectrochemistry

The spectroelectrochemical properties were examined by analyzing the UV/Vis/NIR spectra of films treated at different oxidization conditions. These experiments were carried out by both CV and chronoamperometry, using the KClO<sub>4</sub> solution. The results are shown as a series of electronic spectra correlated to films electrochemically treated (Figure 7).

760

Thus, prior to anodic treatment, the white-yellowish films showed an intense band at 335 nm, with lack of additional absorptions all along the visible region (Figure 7A). A negligible absorbance increasing between 400 and 600 nm was observed after multicycling the LB film (3 times) up to 0.7 V (Figure 7B), potential value ascribed to the anodic wave rising previous to peaking (i.e. earlier than complete oxidization of m-MTDATA). On the other hand, by further increasing the applied potential to 1.3 V and 1.6 V, the film turned greenish and displayed new absorption patterns near 450 nm, such a band ascribed to the formation of radical species, besides a wide-ranging band growing from ca. 760 nm, which is markedly extended

780

over NIR region (Figures 7C-D). At 1.3 V, this band shows a maximum at 910 nm, which is more intense and slightly red-shifted when oxidizing up to 1.6 V. These emerging bands are due to the formation of new species at the film's surface during its oxidization, namely aminyl radical cations. Afterwards, and as a stronger oxidization method, chronoamperometry was applied to overoxidize the film – submitting it to 2.5 V during a period of 15 s –. Then, it was observed how the NIR absorption even increased noticeably, further modifying its shape. Moreover, the band emerging at 448 nm, related to the radical nature of the film-forming material, diminished drastically (Figure 7E), whereas that with maximum at 335 nm showed no change. Overall, the appearance of this intense and well-separated band located at NIR is in agreement with the occurrence of Intervalence Charge Transfer (IVCT) between two redox centers in the film-forming molecule<sup>18,25,33</sup>. By monitoring the NIR's absorption upon each oxidization, it can be deduced that the IVCT excitation changes (figures 7C to 7E) both in energy, intensity and shape (bandwidth). This trend suggests that the molecule's reorganization energy and coupling between redox centers<sup>25</sup> are modified, then varying the transition's features between ground and excited states in the material.

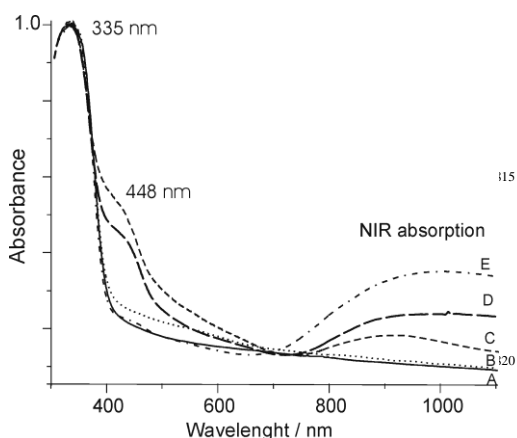


**Fig.7.-** Spectroelectrochemical behavior of m-MTDATA LB films at different oxidization stages: A) as-grown film; B) film oxidized up to 0.7 V by CV (three scans); C) analogous treatment up to 1.3V; D) up to 1.6 V; E) after

submitting the film to Chronoamperometry (at 2.5 V during 15 s).

According to the proposed oxidization mechanism, after oxidization, we are creating positive charges (i. e. holes, p-doping by electrochemistry) that are supposed to diffuse all along the packed film, a process favored by the insertion of electrolyte's counteranions, which stabilize the formed radical species (by chemical reaction). The electrolyte's stabilization was supported by the irreversible tendency of the optical features when performing the electroreduction of the films. The concurrent formation of "polymeric" structures from m-MTDATA cannot be discarded, taking into consideration the known affinity between radical species and the trend followed by the band at ca. 450 nm throughout the progressive oxidization process showed in Figure 7 (a transient process from neutral to radical, and then polymeric species).

Thus, this particular phenomenon is integrated with the fact that  $\pi$ -bridged triphenylamine derivatives are very functional hole carrier systems, since they showed coupling of redox centers over  $\pi$ -conjugated channels in thin molecular films is a key factor on the design of new optoelectronic materials<sup>34</sup>.

## Conclusions

The fabrication of Langmuir and Langmuir-Blodgett films of a non-amphiphilic starburst molecule as m-MTDATA has been attained for first time ever. The  $\Pi$ -A isotherms of the floating layer of m-MTDATA indicated the formation of an extended solid phase, and the successive compression-expansion cycles revealed that despite the fact that it is not a monomolecular floating layer, the Langmuir film presented strong cohesion, not high film rigidity and a good stability. These characteristics allowed the transfer onto solid substrates, accomplishing uniform films. The FT-IR analysis showed that the films exhibit an isotropic nature but with an enhanced molecular planarity due to the induced packing by the use of the LB technique. On the other hand, the solid state electrochemistry and spectroelectrochemistry highlighted the strong

electron donating character of m-MTDATA. Meanwhile in solution two oxidation processes involving one-electron releasing took place ascribed to interacting triphenylamine centers, but in LB solid state only one peak is observed, suggesting the formation of an equivalent radical cationic derivative stabilized by delocalization all along the packed film. The electrolyte's anions influence markedly the redox mechanism. It is believed to consist of a local ion-pair formation at the surface, being stronger in case of Cl<sup>-</sup>-aq. For ClO<sub>4</sub><sup>-</sup>-aq, due to its lower hydration energy (i.e. hydrophobicity) its diffusion into the film is facilitated. The spectroelectrochemical measurements showed that the oxidized species exhibit new absorption features, being of special interest the emerging bands in the NIR region. The features of this band (energy, intensity and shape) depended on the extent of the oxidization performed. According to the mixed-valence nature of m-MTDATA, this excitation is attributed to an intermolecular intervalence charge transfer (IVCT) between the formed aminyl radical cations. The charge transfer is believed to be assisted by the molecular thin film state (pure intermolecular interactions; electroless formed film). The stabilization of the oxidized material is favored by the above-concluded insertion of counterions, then making irreversible the electroreduction process. Finally, the transient formation of polymeric species at higher potentials cannot be completely discarded.

### Acknowledgements

The GOODFOOD program (FP6-1-508774-IP) is grateful acknowledged for the financial support.

### Notes and references

- 1 C. W. Tang, *Appl. Phys. Lett.* 1986, 48, 183.
- 2 J. H. Burroughes, D. D. C. Bradley, A. R. Brown, R. N. Marks, K. Mackay, R. H. Friend, P. L. Burn, A. B. Holmes, *Nature* 1990, 347, 539.
- 3 P. Peumans, A. Yakimov, S. R. Forrest, *J. Appl. Phys.* 2003, 93, 3694.
- 4 a) Y. Shirota, *J. Mater. Chem.* 2000, 10, 1; b) Y. Shirota, *J. Mater. Chem.* 2005, 15, 75.

- 5 K. Itano, H. Ogawa, Y. Shirota, *Appl. Phys. Lett.* 1998, 72, 636.
- 6 T. Noda, H. Ogawa, Y. Shirota, *Adv. Mater.* 1999, 11, 283.
- 7 M. Ishihara, K. Okumoto, Y. Shirota, *Proc. SPIE- Int. Soc. Opt. Eng.* 2004, 5214, 133.
- 8 M. C. Petty, *Langmuir-Blodgett Films. An Introduction*; Cambridge University Press: Cambridge, 1996.
- 9 S. V. Mello, A. Dhanabalan, O. N. Jr. Oliveira, *Synth. Met.* 1999, 102, 1433.
- 10 J. F. Nierengarten, J. F. Eckert, Y. Rio, M. D. Carreon, J. L. Gallani, D. Guillon, *J. Am. Chem. Soc.* 2001, 123, 9743.
- 11 A. Riul Jr., L. H. C. Mattoso, S. V. Mello, G. D. Tellesa, O. N. Jr. Oliveira, *Synth. Met.* 1995, 71, 2067.
- 12 M. L. Rodríguez-Méndez, J. Souto, J. De Saja-González, J. A. De Saja, *Sens. Actuators B: Chem.* 1996, 31, 51.
- 13 D. Russell, R. Meyer, N. Jubran, Z. Tokarski, R. Moudry, K. Law, *J. Electroanal. Chem.* 2004, 567, 19.
- 14 V. Parra, T. Del Caño, M. L. Rodríguez-Méndez, J. A. De Saja, R. F. Aroca, *Chem. Mater.* 2004, 16, 358.
- 15 T. Johansson, W. Mammo, M. Svensson, M. R. Andersson, O. Inganäs, *J. Mater. Chem.* 2003, 13, 1316.
- 16 Y. Shirota, T. Kobata, N. Noma, *N. Chem. Lett.* 1989, 1145.
- 17 M. Thelakkat, H. -W. Schmidt, *Adv. Mater.* 1998, 10, 219.
- 18 M.-Y. Chou, M.-K. Leung, Y. O. Su, C. L. Chiang, C. -C. Lin, J. -H. Liu, C. -K. Kuo, C. -Y. Mou, *Chem. Mater.* 2004, 16, 654.
- 19 M. I. Ranasinghe, O. P. Varnavski, J. Pawlas, S. I. Hauck, J. Louie, J. F. Hartwig, T. Goodson, *J. Am. Chem. Soc.* 2002, 124, 6520.
- 20 a) M. B. Robin, P. Day, *Adv. Inorg. Chem. Radiochem.* 1967, 10, 247; b) K. D. Demadis, C. M. Hartshorn, T. J. Meyer, *Chem. Rev.* 2001, 101, 2655.
- 21 C. Lambert, G. Nöll, *Synth. Met.* 2003, 139, 57.
- 22 V. Parra, T. del Caño, S. Coco, M. L. Rodríguez-Méndez, J. A. De Saja, *Surf. Sci.* 2004, 550, 106.

- 
- <sup>975</sup> 23 P. A. Chollet, J. Messier, C. Rosilio, J.  
Chem. Phys. 1976, 64, 1042.
- 24 J. Rabolt, F. C. Burns, N. E. Schlotter, J.  
D. Swalen, J. Chem. Phys. 1983, 78, 946.
- 25 T. Del Caño, R. Aroca, J. A. De Saja, M.  
<sup>980</sup> L. Rodríguez-Méndez, Langmuir 2003, 19, 3747.
- 26 a) G. Casalbore-Miceli, A. Degli Esposti,  
V. Fattori, G. Marconi, C. Sabatini, Phys. Chem.  
Chem. Phys. 2004, 6, 3092; b) A. Degli Esposti,  
V. Fattori, G. Casalbore-Miceli, G. Marconi,  
<sup>985</sup> Phys. Chem. Chem. Phys. 2005, 7, 3738.
- 27 C. Lambert, G. Nöll, J. Am. Chem. Soc.  
1999, 121, 8434.
- 28 G. Valincius, G. Niaura, B.  
Kazakevičiene, Z. Talaikyte, M. Kažemekaite, E.  
<sup>990</sup> Butkus, V. Razumas, Langmuir 2004, 20, 6631.
- 29 N. V. Rees, J. D. Wadhawan, O. V.  
Klymenko, B. A. Coles, R. G. Compton, J.  
Electroanal. Chem. 2004, 563, 191.
- 30 C. Lambert, G. Nöll, Angew. Chem. Int.  
<sup>995</sup> Ed. 1998, 121, 8434.
- 31 C. -H. Chen, J. -W Shen, K. Jakka, C. -  
F. Shu, Synth. Met. 2004, 143, 215.
- 32 R. A. Marcus, N. Sutin, N. Biochim.  
Biophys. Acta 1985, 811, 265.
- <sup>1000</sup> 33 A. Knorr, J. Daub, Angew. Chem. Int.  
Ed. Engl. 1997, 36, 2817.
- 34 P. M. Borsenberger, D. S. Weiss, Organic  
Photoreceptors for Imaging Systems; Marcel  
Dekker: New York, 1993.

<sup>1005</sup>

<sup>1010</sup>

---

